Supplementary Material

1 UAV COMPONENTS AND LAYOUT

We have listed the mechanical and electronic components we have used to assemble our UAV in Table S1 and sketched the layout of the UAV with the position of all the components in Figure S1.

Component	**Reference**	**Price** (USD)
Fixed wing body	X8 Skywalker	300
Motor	Scorpio SII-4020-420 KV	135
Controler	Castle Phoenix Edge 50A regler	100
Servo motors	2 × DES 678 BB MG servo	80
Propellers	Aeronaut CAMcarbon 17”x9”	20
Autopilot	Pixhawk HKPILOT 32	200
GPS	UBLOX NEO-M8N GPS	50
Telemetry	HKPILOT 500MW Telemetry	50
Air speed sensor	HKPILOT 32 digital air speed	50
Lidar	Lightware SF10/A	300
RC receiver-sender	Futuba T14SG-R7008SB	640
Battery	2 × 4S5P 16Ah Li-Ion (Panasonic NCR18650B cell)	500
Camera	Sony α6000 with 16mm Sony SEL16F29 lens	800
Camera trigger release	Sony α6000 trigger cable	35
GNSS receiver	2 × Emlid Reach (base and rover)	600
Hot shoe cable	Tuffwing/Reach hot shoe cable	80
Total price		3940

Table S1. List, reference and cost of UAV components.

2 AUTOPILOT PARAMETER TUNNING

The most important parameters we have changed from the default ones coming with arduplane 3.5.3 are listed in Table S2. The parameters we have tunned to get an energetically-efficient platform were:

- The PID parameters controlling the flight stability – i.e. those necessary to control the roll, pitch and yaw response of the fixed-wing – were tuned by following the “autotune” procedure, which automatically optimizes the parameters by flying a sequence of sharp maneuvers, and retaining the parameters that yield to the most stable flight.
- The parameters of the navigation controller – which ensure smooth flight trajectory while preventing too aggressive navigation (sharp corners) – were tuned by field testing.
- The parameter of the air speed sensor (pitot tube) was calibrated by flying a sequence of circles (the mean air and ground speeds being the same on average irrespective of the wind speed). This tuning is crucial to estimate the air speed accurately, and then to ensure the fixed-wing to fly slightly above the stall speed, which is optimal as it minimizes the drag and thus also minimizes the energy consumption.
- The stall speed was estimated and set to 12 m s^{-1}. This parameter essentially serves to trigger a stall prevention procedure in case the air speed drops below this value.

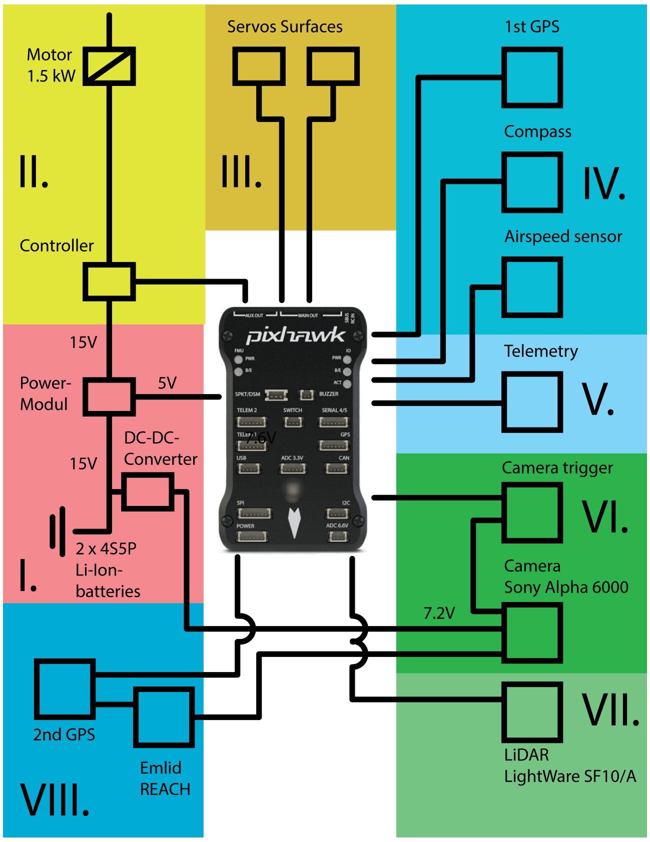

Figure S1. Layout of the UAV components around the Pixhawk autopilot.

- The cruise speed – i.e. the air speed the autopilot targets to achieve during any mission in flight level – was set to 16 m s^{-1}, which was found to be a good trade-off between flight efficiency and safety (with enough margin from the stall speed).

3 TAKE-OFF WITH BUNGEE

The fixed-wing was installed on a 2 m-long and $15°$-inclined ramp anchored to the ground before taking-off. The bungee system consists of an elastic rope (that provides the thrust to catapult the plane until it can fly on its own) attached to a Y-shaped non-elastic rope. One side of the Y-shaped rope is attached to the plane via a hook fixed underneath. The other side is attached to the ground through a releaser that serves for triggering the take-off. The plane's hook must be located in front of the center of gravity to ensure stable take-off. For successful take-off, it was crucial to adjust the tension of the bungee: it should be sufficient to give enough initial thrust, but not too much to prevent uncontrollable behaviors. We found that $\sim$30 kg gave the best results providing an initial maximal velocity of $\sim$25 m s^{-1}. In automatic take-off mode, the autopilot detects the initial thrust (from velocity and acceleration data) and orders full throttle of the motor once the first motion is detected, keeping the fixed-wing leveled until reaching a predefined altitude (we used 50 m) before switching to the first waypoint loaded in the mission command. To prevent the bungee from colliding with the spinning propeller, we imposed a 2-second delay between the detection of the first motion and the motor start. The bungee and the UAV were always oriented against the wind to ensure sufficient air speed for take-off and limit the dangerous effects of cross-winds.

Parameters	Value	Description
AHRS_EKF_TYPE	1	Use Extended Kalman Filter (EKF) algorithm to estimate vehicle position, velocity and angular orientation based on instrument data
ARSPD_FBW_MIN	13	Set the stall speed to 13 m s^{-1}
BATT_CAPACITY	32000	Set the battery capacity to 32Ah
CAM_TRIGG_TYPE	1	Allow the autopilot to trigger the camera
EKF_ENABLE	1	Activate 'EKF1' (see AHRS_EKF_TYPE)
EKF2_ENABLE	0	Deactivate 'EKF2' (see AHRS_EKF_TYPE)
LIM_ROLL_CD	4000	Limit roll to 40 °
MAG_ENABLE	0	Deactivate the use of the compass for navigation
MIN_GNDSPD_CM	500	Set the minimum ground speed to 5 m s^{-1}
NAVL1_PERIOD	27	Define a type of UAV navigation from gentle (large turns) to aggressive (sharper corners)
RTL_AUTOLAND	2	Use a landing sequence if the mode 'Return To Launch' is activated
TECS_LAND_ARSPD	16	Define the target air speed at landing to 16 m s^{-1}
TECS_LAND_SPDWGT	0	Define a landing parameter
TKOFF_THR_DELAY	20	Set a 2 s delay between the first motion is detected and the motor start at take-off
TKOFF_THR_MINACC	15	Detect first motion when the acceleration exceeds 15 m s^{-1}/s
TKOFF_THR_MINSPD	4	Detect first motion when the speed exceeds 4 m s^{-1}
TRIM_ARSPD_CM	1600	Set the target cruise air speed to 16 m s^{-1}
WP_RADIUS	100	Set a tolerance to accept the achievement of waypoints

Table S2. Parameters changed from the default ones of arduplane 3.5.3 (see `http://ardupilot.org/ardupilot` for further information about the meaning of each parameter).

4 NET LANDING

We used a 20 x 5 m net with 1 cm mesh size attached along two 6-meter-long telescopic aluminum masts to smoothly catch the UAV during the final approach before it touches the ground. The UAV was programed to hit the net automatically by placing the last waypoint ∼20 m behind the net. While the UAV was capable of reaching the last waypoint horizontally within a few meters, its vertical positioning was found too inaccurate for fully automatizing the net landing. Indeed, the altitude positioning relies on a barometer, whose precision decreases with flight time (e.g. the air pressure might change in a few hours if the weather changes). As a remedy, we equipped our UAV with a Lidar to estimate the distance to the ground during the landing phase. While the technique improved the chance to land automatically into the net, it could not cover all the wind configurations, and pilot inputs (overriding the programmed trajectory) were sometimes needed to correct the landing slope and successfully reach the net. Advantageously, the net landing technique proved to be efficient irrespectively of the wind direction, and fast landing (ground speed up to 25 m s^{-1}) were realized without damaging the UAV.

5 MISSION DATA

Table S3 gathers together key fight data (distance traveled, flight duration, battery consumption) of all the UAV missions operated in the Inglefield Bredning (July 2017) and at Eqip Sermia Glacier (July 2018).

6 SFM-MVS PROCESSING

The UAV images collected during the surveys were processed by Structure-from-Motion Multi-View Stereo (SfM-MVS) using the software Agisoft PhotoScan v1.4.3. Computations were performed on a working

Year	Mission	Date	Take-off time (UTC)	Traveled dist. (km)	Flight alt. (m a.s.l.)	Duration (hour)	Battery cons. (Ah)
2017	Red	July 5	18:00	151	829	2.67	17
2017	Blue	July 5	23:37	192	805	-	-
2017	Red	July 6	16:12	151	806	2.78	17.9
2017	Blue	July 7	00:07	165	828	3.06	19.4
2017	Red	July 7	16:10	166	806	2.96	18.4
2017	Blue	July 7	23:16	165	806	2.8	19.5
2017	Red	July 8	14:01	167	812	2.98	17.4
2017	Blue	July 8	20:26	175	813	3.2	20.2
2017	Red	July 9	15:18	168	802	3.22	18.1
2017	Blue	July 10	00:23	156	817	3.21	20
2017	Red	July 14	12:16	182	822	-	-
2017	Blue	July 14	18:45	181	813	3.04	19.8
2017	Red	July 15	16:57	179	818	2.86	21.6
2017	Blue	July 15	23:02	178	828	3.26	19.3
2017	Red	July 16	12:53	167	823	2.86	16.8
2017	Blue	July 16	19:58	166	801	2.89	19.4
2018	Red	July 7	12:45	168	838	2.74	13.8
2018	Red	July 7	18:00	168	848	2.74	15
2018	Blue	July 8	12:25	173	845	2.77	18.7
2018	Red	July 8	16:10	166	874	2.71	19.5
2018	Blue	July 11	12:24	173	852	2.92	15.1

Table S3. List of all the UAV missions flown during the 2017 and 2018 field campaigns with key flight data. In 2017, blue missions included the survey of Tracy and Heilprin glaciers, while red missions included the survey of Hart, Sharp, Melville, and Farquhar glaciers (Fig. 1). In 2018, red missions consisted of repeat missions focusing on the calving front of Eqip Sermia glacier, while blue missions consisted of a single large-scale survey (Fig. 2).

station equipped with an Intel Xeon CPU E5-2687W v4 3.00GHz processor (24 cores). PhotoScan performs two main steps ('SfM' and 'MVS'), which are now described in turn.

The SfM step includes a feature-detection algorithm to detect "tie points" on every image and an algorithm to match them between the different available views. Here we used the 'Medium' accuracy for this step. The known location of images serves to reduce the processing time as the search for matching points is restricted to neighboring images. The output of this step is a sparse point cloud. A bundle-adjustment algorithm is used to find the parameters of the camera model.

The MVS step consists of matching algorithms that aim to increase the density of the sparse point cloud. Here we used the 'Aggressive' depth filters and parameter 'Medium' to define the cloud quality for building the dense cloud.

Table S4 gives some examples of output data for the processing of two UAV surveys (one in 2017 and one in 2018). It must be stressed that camera location error estimates reported by Agisoft PhotoScan indicate a reduction of the error by factor $\sim$300 after adopting the 2018 method for geo-tagging aerial images.

7 TEMPLATE MATCHING PARAMETERS

Table S5 gives the parameters we have used in ImGRAFT to obtain the ice surface velocity fields displayed in Figures 5, 6, 7 and 10.

8 BATTERY PERFORMANCE

From the log files of the autopilot, we analyzed the battery consumption of our UAV (Fig. S2) during one of the longest flights, which was performed in the Inglefield Bredning in 2017. We found a total consumption

Glacier	Tracy	Eqip Sermia
Surveying date	9 July 2017	11 July 2018
Number of images	1354	2363
Coverage area (km^2)	22.6	49.1
Mean GSD (cm/pixel)	16.2	14.3
Tie points	197,650	532,877
Dense points	80,530,831	211,074,343
Camera XY location error estimates	4.8 m	1.3 cm
Camera Z location error estimates	12.1 m	3 cm
SfM: Matching time	∼3 hours	∼5 hours
SfM: Alignment time	∼21 min	∼29 min
MVS: Depth maps generation time	∼2 days	∼3 days
MVS: Dense cloud generation time	∼7 hours	∼11 hours

Table S4. Output data for the processing of two UAV surveys by SfM-MVS with Agisoft Photoscan.

Figures	5 & 6, left panels	5 & 6, right panels	7	10
Region	Inglefield Bredning	Inglefield Bredning	Eqip Sermia	Eqip Sermia
Source of data	UAV	Sentinel-2A	UAV	UAV
Resolution of data	0.5 m	10 m	1 m	0.25 m
Grid spacing	50 m	50 m	50 m	5 m
Template window size	50 pixel	40 pixel	50 pixel	100 pixel
Search window size	150 pixel	90 pixel	100 pixel	150 pixel

Table S5. Parameters used in ImGRAFT for this study.

of ∼20 Ah, i.e. approx. 100 W in average during the 3 hour-long flight. During this flight, the battery voltage dropped by ∼1 V every hour (from ∼15.5 V to ∼12.8 V), leaving a safe margin. These results are consistent with the discharge curve (given for 1 C) of the Li-ion Panasonic NCR18650B cells at around 0°C (not shown), which indicates a roughly linear drop of voltage from 16 V to 12 V, and non-linear from 12 V to 10 V, which corresponds to full discharge. On the other hand, the log file indicated that the UAV traveled ∼180 km in total. Figure S2 demonstrates that the power capabilities of the UAV exceeded the need of the study, as the UAV could travel up to a maximum of 200 km while keeping the voltage above the safe value of 12 V.

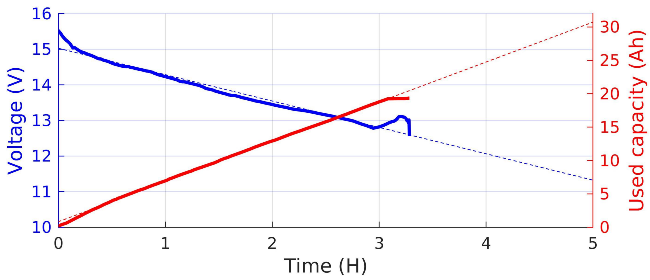

Figure S2. Battery voltage and used capacity during a 180-km long flight operated in the Inglefield Bredning.